

# Evaporation-driven self-organization of sol–gel dip-coating films

Hiroaki UCHIYAMA<sup>†</sup>

Department of Chemistry and Materials Engineering, Kansai University,  
3–3–35 Yamate-cho, Suita, Osaka 564–8680, Japan

In this review, we discuss the spontaneous pattern formation of sol–gel dip coating films induced by solvent evaporation, as a novel patterning technique. Linearly arranged striations and cell-like patterns were obtained upon withdrawing the substrate from the coating solution at increasing withdrawal rates. Such highly ordered micropatterns formed by the Bénard–Marangoni convection mechanism triggered by solvent evaporation. In contrast, dip-coating at rates below  $1.0 \text{ cm min}^{-1}$  generated periodic stripe patterns arranged on the surface of the films that were perpendicular to the substrate withdrawal direction. Such a formation design was attributed to the onset of capillary flow of the coating solution at the meniscus induced by solvent evaporation.

©2015 The Ceramic Society of Japan. All rights reserved.

Key-words : Thin film materials, Sol–gel method, Dip-coating, Surface patterns, Self-organization

[Received March 6, 2015; Accepted March 17, 2015]

## 1. Introduction

Spontaneous pattern formation through self-assembly and self-organization is a practically important and genuinely interesting phenomenon for many researchers in various technological and scientific fields. Spontaneous assembly and organization of molecules, colloids, or particles result in unique and sophisticated micro- and nanopatterns. Many studies have focused on self-assembly and self-organization as alternative fabrication processes for generating highly ordered patterns in thin film materials.<sup>1)–14)</sup> Honeycomb patterns in polymer films were realized by casting polymer solutions under humid conditions.<sup>1)–4)</sup> Periodic stripe patterns were achieved by controlling the wrinkling of the surface of metallic,<sup>5),6)</sup> organic,<sup>7),8)</sup> and organic–inorganic hybrid films.<sup>9),10)</sup> Ordered web-like structures consisting of diblock copolymers were obtained through two consecutive self-assembly processes at different length scales.<sup>11)</sup> Such micron- and nano-patterned films prepared via self-assembly and self-organization have great potentials for practical applications such as electronics, photonics, and biology.

Sol–gel coating techniques are widely used for preparing inorganic and organic–inorganic hybrid films.<sup>15),16)</sup> The synthesis process generally involves the preparation of precursor sols via the hydrolysis and condensation of metal alkoxides, the deposition of amorphous gel films on substrates, and the drying and heating of the gel films. During the deposition process, solvent evaporation from the coating layer occurs, and often involves convective flows of the solutions on the substrate. Such a mechanism results in gel films with uneven thicknesses and rough surfaces. Furthermore, such an evaporation-driven convective flow mechanism operating in sol–gel coating films has been investigated by several approaches, as exemplified. Birnie et al. investigated the coating thickness defects on sol–gel spin-coating films. The striation defects resulted from the Bénard–Marangoni convection mechanism induced by solvent evaporation.<sup>17)–20)</sup> Grosso et al.

prepared sol–gel films by dip-coating using extreme conditions (e.g., ultralow or fast substrate withdrawal speeds and high evaporation rates). The thickness of the dip-coating films prepared using considerably low substrate withdrawal speeds below  $0.01 \text{ mm s}^{-1}$  ( $0.06 \text{ cm min}^{-1}$ ) increased with decreasing substrate withdrawal speeds. Such a phenomenon was caused by the onset of capillary flow of the coating solution induced by solvent evaporation at the edge of the meniscus.<sup>21),22)</sup> Such thickness variations and surface roughening triggered by solvent evaporation are regarded as a self-organization process. Thorough understanding of the evaporation-driven convective flow during coating would enable the development of novel patterning techniques for producing periodic surface patterns on sol–gel coating films.

This review describes novel self-organization techniques of sol–gel dip-coating films based on evaporation-driven convective flow mechanism. First, spontaneous pattern formation induced by Bénard–Marangoni convection is demonstrated. Secondly, evaporation-driven pattern formation during low-speed dip-coating is discussed.

## 2. Evaluation method of surface patterns

Microscopic observation was made on the thin films using an optical microscope (KH-1300, HiROX, Tokyo, Japan). Two- (2D) and three-dimensional (3D) surface profile of the thin films was measured using a contact probe surface profilometer (SE-3500K31, Kosaka Laboratory, Tokyo, Japan). The measurement was conducted at the center of the thin films.

Surface roughness parameters,  $R_z$  (ten point height of irregularities) and  $S$  (mean spacing of local peaks) were calculated from the 2D profile (The definitions of  $R_z$  and  $S$  are shown in Fig. 1).  $R_z$  and  $S$  represent the height and spacing, respectively, of the surface patterns.

Film thickness was measured by the surface profilometer (The definitions of the thickness are shown in Fig. 1). A part of the thin film was scraped off with a surgical knife immediately after the film deposition, and the level difference between the coated part and the scraped part was measured after drying or heating of gel films.

<sup>†</sup> Corresponding author: H. Uchiyama; E-mail: h.uchi@kansai-u.ac.jp

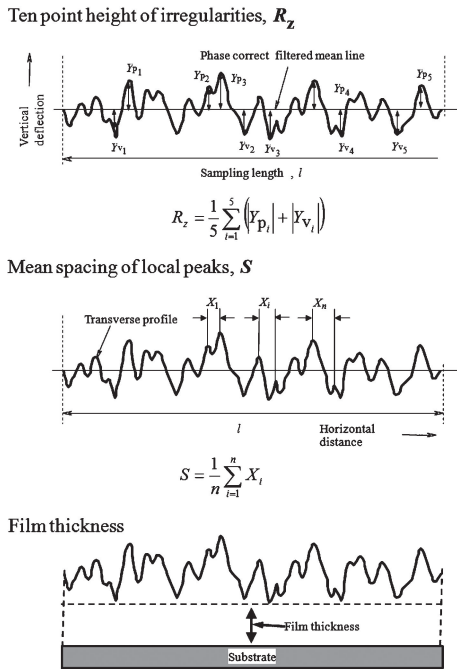


Fig. 1. Surface roughness parameters,  $R_z$  (10 point height of irregularities) and  $S$  (mean spacing of local peaks of the profile), and the definition of film thickness.

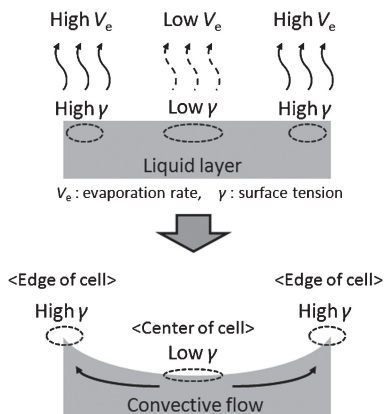


Fig. 2. Schematic illustration of Bénard-Marangoni convection.

### 3. Spontaneous pattern formation induced by Bénard-Marangoni convection

#### 3.1 Spontaneous formation of cell-like patterns induced by Bénard-Marangoni convection

The Bénard-Marangoni convection is schematically shown in Fig. 2. Solvent evaporation from liquid layers often induces a thermal or a compositional gradient on the surface, causing a local increase in surface tension.<sup>23)–28)</sup> The surface tension inhomogeneity leads to convective flows, i.e., Bénard-Marangoni convection, resulting in the formation of cell-like patterns on the surface (i.e., Bénard cell). The Bénard-Marangoni convection can be characterized by the Marangoni number,  $Ma$ , which is a measure of the occurrence tendency of convection, as described below:<sup>23),29)</sup>

$$Ma = \frac{-(\partial\gamma/\partial T)H^2\nabla T}{\mu\alpha} \quad (1)$$

$$Ma = \frac{-(\partial\gamma/\partial C)H^2\nabla C}{\mu D} \quad (2)$$

where  $\partial\gamma/\partial T$  is the temperature derivative of the surface tension,  $\nabla T$  is the temperature gradient near the solution surface,  $\partial\gamma/\partial C$  is the concentration derivative of the surface tension,  $\nabla C$  is the compositional gradient near the solution surface,  $H$  is the thickness of the solution layer,  $D$  is the mass diffusivity of the component, and  $\mu$  and  $\alpha$  are the viscosity and thermal diffusivity of the solution, respectively. Equation (1) is used when the temperature gradient dominates the Marangoni effect, whereas Eq. (2) is employed when the concentration gradient is the main driving force. Generally, Bénard-Marangoni convection occurs when  $Ma$  is high;  $Ma$  increases with increasing thermal or compositional gradients near the solution surface, increasing thicknesses of the solution layer, and decreasing solution viscosities, as shown in Eqs. (1) and (2).

Bénard-Marangoni convection is known as one of the important factors contributing to the thickness variation and surface roughening of sol-gel coating films. More specifically, cell-like Bénard-Marangoni convection occurs in the coating layer on the substrate during solvent evaporation. The surface patterns are then fixed by gelation, generating uneven film thickness. Birnie et al. investigated the formation mechanism of coating thickness defects on sol-gel-derived spin-coating films. The authors showed that striation defects resulted from Bénard-Marangoni convection induced by solvent evaporation during spin-coating.<sup>17)–20)</sup> Kozuka et al. also studied radiative striations on sol-gel-derived spin-coating films. Cell-like patterns formed near the spinning center of the films.<sup>30)–32)</sup> Daniels et al. investigated the formation of radiative striations for spin-on photoresist layers prepared from organic polymer solutions. The authors reported that cell-like Bénard-Marangoni convection distributes along radial lines during spin-coating, leading to the development of radiative striations.<sup>33)</sup> These results suggested that the shape of the surface patterns obtained by Bénard-Marangoni convection depends on the flow direction of the coating solution on the substrate during coating.

The evolution of Bénard-Marangoni convection is also expected to occur on dip-coating films, whereby cell-like convections would linearly arranged during dip-coating owing to the unidirectional flow of the solutions on a substrate by gravity that is opposite to the substrate withdrawal direction. The spontaneous formation of such periodic surface patterns is regarded as a self-organization process that may be useful for preparing functional metal oxide films. The self-organization of sol-gel dip-coated films induced by Bénard-Marangoni convection is described in the following section.

#### 3.2 Effect of substrate withdrawal speed on pattern formation induced by Bénard-Marangoni convection

The effect of the substrate withdrawal speed on the pattern formation induced by Bénard-Marangoni convection was studied on alkoxide-derived titania films.<sup>34)</sup> Starting solutions of  $\text{Ti}(\text{OC}_3\text{H}_7)_4:\text{H}_2\text{O}:\text{HNO}_3:i\text{-C}_3\text{H}_7\text{OH}$  molar composition of 1:2:0.2:60 were prepared and stored at room temperature in a sealed glass container for 3 h. The solutions served as the coating solutions for dip-coating. Gel films were deposited on silica glass substrates (20 mm × 40 mm × 0.85 mm) by dip-coating; the substrates were withdrawn at varying speeds of 1–140 cm min<sup>-1</sup> using a dip-coater (MICRODIP MD-0408, SDI, Kyoto, Japan). Following deposition, the gel films were heated at 600°C for 10 min.

Transparent, crack-free titania films were obtained irrespective of the substrate withdrawal speed. The film thickness increased from ca. 30 to ca. 140 nm with increasing substrate withdrawal speeds. Smooth surfaces were obtained at low substrate withdrawal speeds of 1–30  $\text{cm min}^{-1}$  [Fig. 3(a)]. In contrast, linear striations parallel to the substrate withdrawal direction formed on the surface of the films prepared at higher varying speeds of 70–140  $\text{cm min}^{-1}$  [Fig. 3(b)]. Increases in the substrate withdrawal speed led to increases in the height and spacing of the striations (Fig. 4). The height was reduced by heating the gel films at 600°C [Fig. 4(a)]. In contrast, the spacing remained mostly unchanged following heat treatment [Fig. 4(b)].

The linearly arranged striations obtained on the sol-gel dip-coating films may be due to the arrangement and connection of Bénard–Marangoni convective flows along the flow direction of the coating layer. As reported in Section 3.1, striations form via the connection of cell-like Bénard–Marangoni convective flows along the flow direction of the coating layer on the substrate

during coating.<sup>33)</sup> During dip-coating, Bénard–Marangoni convection occurring in the coating layer unidirectionally flows by gravity in a direction opposite to the substrate withdrawal direction, thereby resulting in the formation of linearly arranged striations.

In the present case, linear striations appeared with increasing substrate withdrawal speeds for dip-coating; and the pattern formation was accompanied with increases in the film thickness. As shown in Eqs. (1) and (2),  $Ma$ , which is a measure of occurrence tendency of convection, increased with increasing thicknesses of the coating layer. Thus, increases in the film thickness with increasing substrate withdrawal speeds would generate greater  $Ma$  values, thereby resulting in the formation of linear striations. Moreover, the height and spacing of striations increased with increasing substrate withdrawal speeds. Bénard–Marangoni convection as the source of striation formation is expected to become larger in thicker fluid layer.<sup>30),31)</sup> Thus, increases in the film thickness could lead to the formation of larger striations.

### 3.3 Effect of viscosity of coating solution on pattern formation induced by Bénard–Marangoni convection

The pattern formation induced by Bénard–Marangoni convection is also influenced by the viscosity of the coating solutions. In this section, the effect of the viscosity of the coating solution on the surface pattern of sol-gel dip-coating films is discussed.<sup>34)</sup> The viscosity of the coating solution was controlled by the addition of poly(vinylpyrrolidone) (PVP). Starting solutions of molar compositions,  $\text{Ti}(\text{OC}_3\text{H}_7)_4:\text{H}_2\text{O}:\text{HNO}_3:i\text{-C}_3\text{H}_7\text{OH}:\text{PVP} = 1:2:0.2:60:x$  ( $x = 0\text{--}0.7$ ), were prepared and stored at room temperature in a sealed glass container for 3 h, and served as the coating solutions for dip-coating. Gel films were deposited on silica glass substrates (20 mm  $\times$  40 mm  $\times$  0.85 mm) by dip-coating. The substrates were withdrawn at 70  $\text{cm min}^{-1}$  using a dip-coater (MICRODIP MD-0408, SDI, Kyoto, Japan). Following deposition, the gel films were heated at 600°C for 10 min to obtain titania films.

The viscosity of the coating solution increased from 2.81 to 41.1 mPa with increasing PVP contents ( $x$ ). Transparent, crack-free titania films were obtained for all studied solutions with  $x = 0\text{--}0.7$ . Increase in the solution viscosity led to increased film thicknesses from ca. 80 to ca. 300 nm. Linear striations were observed for the titania films prepared in the absence of PVP

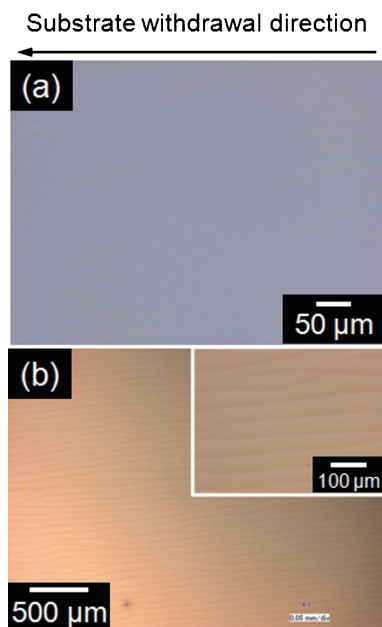


Fig. 3. Optical images of titania films prepared at different substrate withdrawal speeds of (a) 10 and (b) 70  $\text{cm min}^{-1}$ . Reproduced with permission from Ref. 34. Copyright 2010 American Chemical Society.

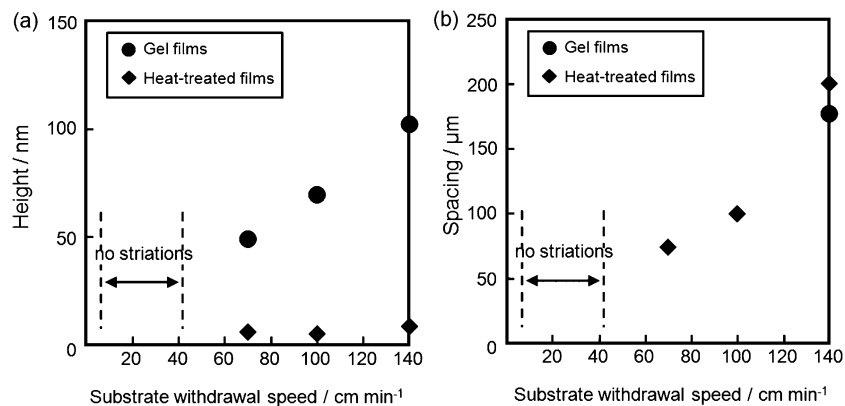


Fig. 4. Dependence of the (a) height and (b) spacing on the substrate withdrawal speed for titania gel and heat-treated films prepared at varying substrate withdrawal speeds of 1–140  $\text{cm min}^{-1}$ . Reproduced with permission from Ref. 34. Copyright 2010 American Chemical Society.

( $x = 0$ ) [Fig. 3(b)]. In contrast, cell-like patterns appeared on the surface of the films prepared in the presence of PVP ( $x = 0.1$ – $0.7$ ), and the cells linearly arranged parallel to the substrate withdrawal direction (Fig. 5). Increases in the PVP content led to increases in the height and width of the cell-like patterns (Fig. 6). The height of the striations decreased upon heat treatment at  $600^\circ\text{C}$  [Fig. 6(a)], whereas the spacing remained unchanged [Fig. 6(b)].

The pattern changed from linear striations to linearly arranged cells with increasing coating solution viscosities (Fig. 6). The higher solution viscosity could suppress the connection of cell-like convections, thereby resulting in the linear arrangement of cells instead of striations. Furthermore, the higher solution viscosity resulted in the formation of larger cell-like patterns that could be attributed to the larger film thickness provided by the higher viscosity.

### 3.4 Effect of coating temperature on pattern formation induced by Bénard–Marangoni convection

The coating temperature i.e., the temperature of the substrate, solution, or atmosphere is expected to influence Bénard–Marangoni convection induced by solvent evaporation. The effect of the coating temperature was studied on silica–PVP hybrid films.<sup>35</sup> Starting solutions of  $\text{Si}(\text{OCH}_3)_4\text{:H}_2\text{O:HNO}_3\text{:CH}_3\text{OCH}_2\text{CH}_2\text{OH:PVP}$  molar composition of 1:2:0.01:14.8:0.7 were prepared and stored at room temperature in a sealed glass container for 30 min, and served as the coating solutions for dip-

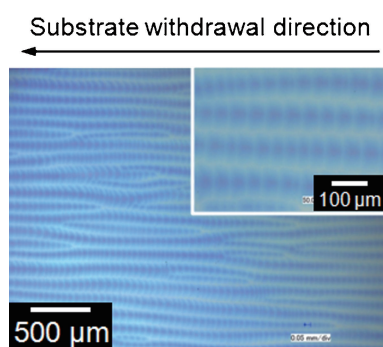


Fig. 5. Optical image of the titania film prepared from coating solution with  $x = 0.3$  at a substrate withdrawal speed of  $70\text{ cm min}^{-1}$ . Reproduced with permission from Ref. 34. Copyright 2010 American Chemical Society.

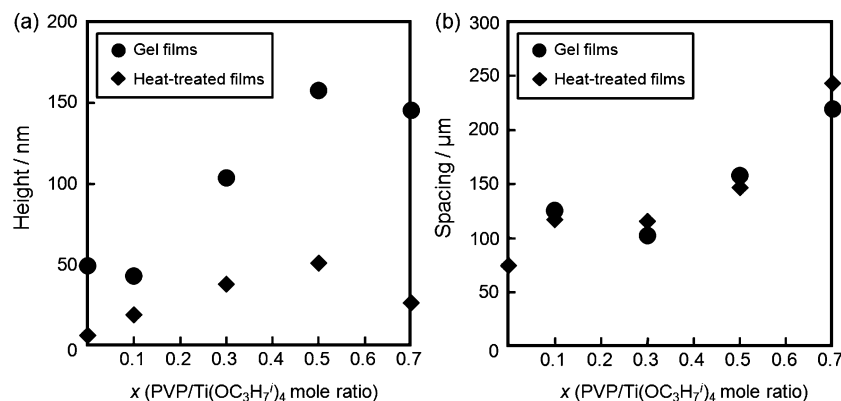


Fig. 6. Dependence of the (a) height and (b) spacing on the PVP/Ti(OC<sub>3</sub>H<sub>7</sub>)<sub>4</sub> mole ratio of the coating solution for the titania gel and heat-treated films prepared at a substrate withdrawal speed of  $70\text{ cm min}^{-1}$ . Reproduced with permission from Ref. 34. Copyright 2010 American Chemical Society.

coating. Silica–PVP films were deposited on Si(100) substrates ( $20\text{ mm} \times 40\text{ mm} \times 0.85\text{ mm}$ ) by dip-coating at a substrate withdrawal speed of  $50\text{ cm min}^{-1}$  using a dip-coater (PORTABLE DIP COATER DT-0001, SDI, Kyoto, Japan) in a thermostatic oven at varying temperatures of  $25$ – $100^\circ\text{C}$ . The solution and substrate were heated at the prescribed temperature for 30 min before dip coating. Following deposition, the thin films were maintained at the coating temperature ( $25$ – $100^\circ\text{C}$ ) for 3 min in the thermostatic oven and then at room temperature for 24 h in air.

Transparent, crack-free silica–PVP hybrid films were obtained under the conditions studied. The film thickness increased from ca.  $2.7$  to ca.  $7.1\text{ }\mu\text{m}$  with increasing coating temperatures. Smooth surfaces were observed for the films prepared at  $25^\circ\text{C}$ . In contrast, linearly arranged cell-like patterns of  $100$ – $200\text{ }\mu\text{m}$  in width formed on the surface of the films prepared at temperatures above  $40^\circ\text{C}$  [Fig. 7(a)]. The three-dimensional surface profiles of the films show that the center of the cells was depressed [Fig. 7(b)]. The height of the cells drastically increased with increasing coating temperatures from  $25$  to  $40^\circ\text{C}$ , and remained mostly unchanged at temperatures above  $40^\circ\text{C}$  [Fig. 8(a)]. Conversely, the width of the patterns decreased with increasing coating temperatures [Fig. 8(b)].

The decrease in the width of the cell-like patterns with increasing coating temperatures [Fig. 8(b)] could be due to the onset of Bénard–Marangoni convection. Higher coating temperatures promote the development of Bénard–Marangoni convection that would result in increases in the number of the convections per unit volume, thus leading to the formation of narrower surface patterns. Conversely, the constant height of the patterns obtained at temperatures above  $40^\circ\text{C}$  [Fig. 8(a)] can be explained as follows. Typically, the onset of Bénard–Marangoni convection at higher temperatures promotes local surface elevation via convective flows that leads to increases in the height of the surface patterns. However, in the case of sol–gel films, the higher temperatures also lead to faster gelation of the coating layer owing to the higher evaporation rates. Hence, the faster gelation can rapidly fix the surface patterns on the coating layer, thereby suppressing further surface elevation.

## 4. Spontaneous pattern formation during low-speed dip-coating

### 4.1 Preparation of sol–gel films by low-speed dip-coating

Dip-coating is widely accepted as a typical deposition method for the preparation of amorphous gel films on a substrate,

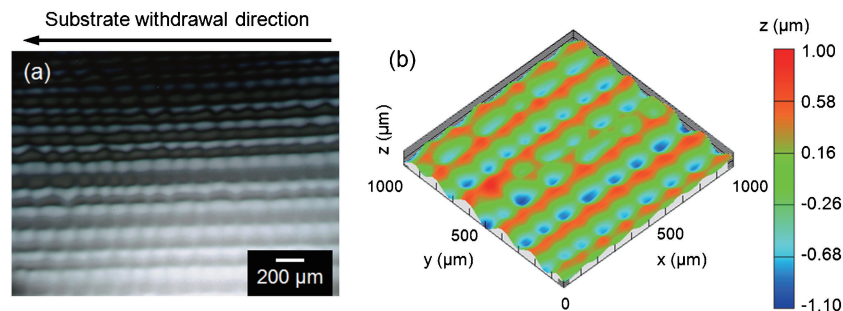


Fig. 7. (a) Optical image and (b) three-dimensional surface profile of the silica-PVP hybrid film prepared at a substrate withdrawal speed of  $50 \text{ cm min}^{-1}$  in a thermostatic oven at  $100^\circ\text{C}$ . Reproduced with permission from Ref. 35. Copyright 2012 American Chemical Society.

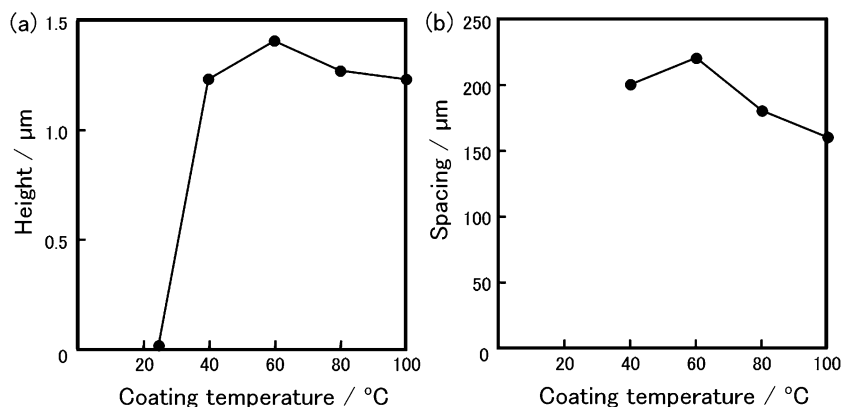


Fig. 8. Dependence of the (a) height and (b) spacing on the coating temperature for the silica-PVP hybrid films prepared at a substrate withdrawal speed of  $50 \text{ cm min}^{-1}$  in a thermostatic oven at varying temperatures of  $25\text{--}100^\circ\text{C}$ . Reproduced with permission from Ref. 35. Copyright 2012 American Chemical Society.

whereby the substrate is dipped into the coating solution and then vertically withdrawn at constant speeds. The thickness of dip-coating films is determined by the equilibrium between the adhesion of the coating solution on the substrate and the gravity-induced viscous drag. Typically, the thickness of dip-coating films increases with increasing substrate withdrawal speeds.<sup>36)</sup> However, Grosso et al. demonstrated that the thickness of sol-gel dip-coating films prepared using considerably low substrate withdrawal speeds below  $0.01 \text{ mm s}^{-1}$  ( $0.06 \text{ cm min}^{-1}$ ) increases with decreasing substrate withdrawal speeds that is due to the onset of capillary flow of the coating solution induced by solvent evaporation at the meniscus.<sup>21),22)</sup> During dip-coating at such low substrate withdrawal speeds, the solvents evaporate from the meniscus, after which the coating solution raises to the edge of the meniscus by capillary forces. Consequently, the edge of the coating solution is pinned to the substrate, and thus the downward flow of the solution by gravity is suppressed, leading to the formation of thicker films. Such a pinning phenomenon of solutions owing to capillary flows is often observed at the edge of droplets of colloidal suspensions where solvent evaporation occurs, and is commonly known as the coffee-ring effect.<sup>37),38)</sup> The capillary flow of the coating solution during low-speed dip-coating has not been thoroughly discussed. We can thus expect that such a unique self-organization can take place under such extreme conditions.

Recently, we reported the preparation of alkoxide-derived dip-coating films by low-speed dip-coating at speeds below  $1.0 \text{ cm min}^{-1}$ . Linear stripe patterns arranged perpendicular to the substrate withdrawal direction formed spontaneously on the

surface of the films.<sup>39)–41)</sup> Such a spontaneous pattern formation during low-speed dip-coating presents a novel fabrication process for the fabrication of highly ordered patterns in thin film materials. Such surface structures thus obtained hold great promise for application in optical devices such as diffraction gratings and microlens arrays. In the following section, the spontaneous pattern formation on sol-gel films prepared by low-speed dip-coating is described.

#### 4.2 Effect of substrate withdrawal speed on pattern formation during low-speed dip-coating

The effect of the substrate withdrawal speed on the pattern formation during low-speed dip-coating was studied on alkoxide-derived silica-PVP hybrid films.<sup>39)</sup> Starting solutions of  $\text{Si}(\text{OCH}_3)_4\text{:H}_2\text{O:HNO}_3\text{:C}_2\text{H}_5\text{OH:PVP}$  molar composition of  $1\text{:}2\text{:}0.01\text{:}20\text{:}0.5$  were prepared and stored at room temperature in a sealed glass container for 30 min, and served as the coating solutions for dip-coating. Gel films were deposited on silica glass substrates ( $20 \text{ mm} \times 40 \text{ mm} \times 0.85 \text{ mm}$ ) by dip-coating; the substrates were withdrawn at varying speeds of  $0.020\text{--}1.0 \text{ cm min}^{-1}$  using a dip-coater (MICRODIP MD-0408, SDI, Kyoto, Japan). Following deposition, the gel films were kept at room temperature for 30 min.

Transparent, crack-free silica-PVP hybrid films were obtained irrespective of the substrate withdrawal speed. The film thickness increased from ca.  $0.85$  to ca.  $8.0 \mu\text{m}$  with decreasing substrate withdrawal speeds. The film prepared using a substrate withdrawal speed of  $1.0 \text{ cm min}^{-1}$  featured a smooth surface with inhomogeneities, as inferred by the interference color pattern

[Figs. 9(a) and 9(b)]. In contrast, stripe patterns perpendicular to the substrate withdrawal direction formed on the surface of the films prepared at varying speeds of 0.020–0.30  $\text{cm min}^{-1}$ . Such a pattern formation was also confirmed by the wavy pattern in the transverse profile [Figs. 9(c) and 9(d)]. Decrease in the substrate withdrawal speed led to increases in the height and spacing of the stripe patterns (Fig. 10).

The formation of linear stripe patterns at low substrate withdrawal speeds could be caused by the stick-slip motion owing to the onset of capillary flow of the coating solution. As mentioned in Section 4.1., during low-speed dip-coating, solvents evaporate from the meniscus, and then the coating solution raises to the edge of the meniscus by capillary forces, resulting in the pinning of the solution to the substrate. Such a pinning phenomenon owing to capillary flow often leads to the formation of periodic patterns through successive pinning of the viscous solution at its edge, and is termed stick-slip motion.<sup>14),42)–51)</sup> The pattern formation mechanism induced by stick-slip motion is schematically shown in Fig. 11. First, gelation of the coating solution locally proceeds at the edge of the meniscus owing to solvent evaporation. Then, the coating solution is continuously supplied to the edge of the meniscus by capillary forces during solvent evaporation. Consequently, the thickness of the coating

layer locally increases at the edge of the meniscus, leading to the formation of a convex gel part. The convex part is continuously raised upon substrate withdrawal, and progressively separates from the meniscus. As a result, the edge of the coating solution moves downward similarly to a receding tide until the next pinning occurs by capillary flow. The linear stripe patterns perpendicular to the withdrawal direction can thus form through successive pinning of the coating solution at the edge of the meniscus and formation of the convex parts owing to the gelation of the solution.<sup>39)</sup>

The height and spacing of the linear patterns increased with decreasing withdrawal speeds (Fig. 10). At low substrate withdrawal speeds, the gelled part at the edge of the meniscus is maintained near the surface of the coating solution for a long time. As a result, it is continuously in contact with sufficient amounts of solution through capillary flow, thereby resulting in increases in the size of the patterns.

#### 4.3 Effect of coating temperature on pattern formation during low-speed dip-coating

The spontaneous pattern formation induced by the capillary flow of solutions triggered by solvent evaporation is expected to be significantly influenced by the coating temperature (i.e., the temperature of the substrate, solution, or atmosphere). The effect of the coating temperature was studied on silica–PVP hybrid films.<sup>41)</sup> Starting solutions of  $\text{Si}(\text{OCH}_3)_4\text{:H}_2\text{O:HNO}_3\text{:CH}_3\text{OCH}_2\text{CH}_2\text{OH:PVP}$  molar composition of 1:2:0.01:14.8:0.5 were prepared and stored at room temperature in a sealed glass container for 30 min, and served as the coating solutions for dip-coating. Silica–PVP films were deposited on Si(100) substrates (20 mm × 40 mm × 0.85 mm) by dip-coating at a substrate with-

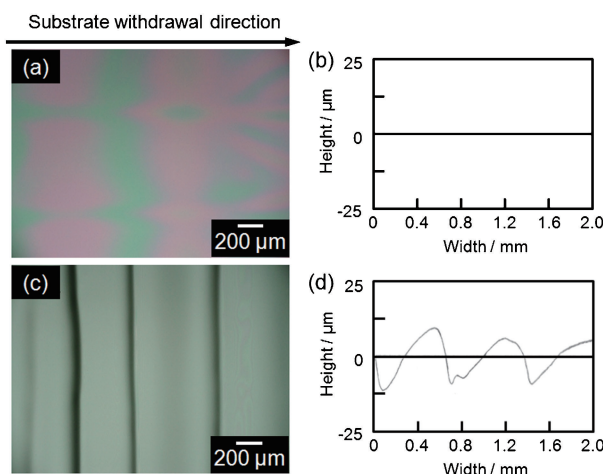


Fig. 9. Optical images and corresponding transverse profiles of the silica–PVP hybrid films prepared at substrate withdrawal speeds of (a, b) 1.0 and (c, d) 0.050  $\text{cm min}^{-1}$ . Reproduced from Ref. 39 with permission from The Royal Society of Chemistry.

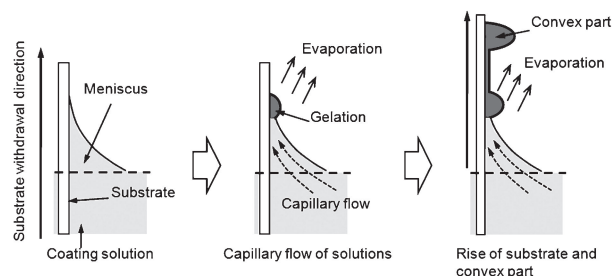


Fig. 11. Schematic illustration of the pattern formation induced by stick-slip motion. Reproduced from Ref. 39 with permission from The Royal Society of Chemistry.

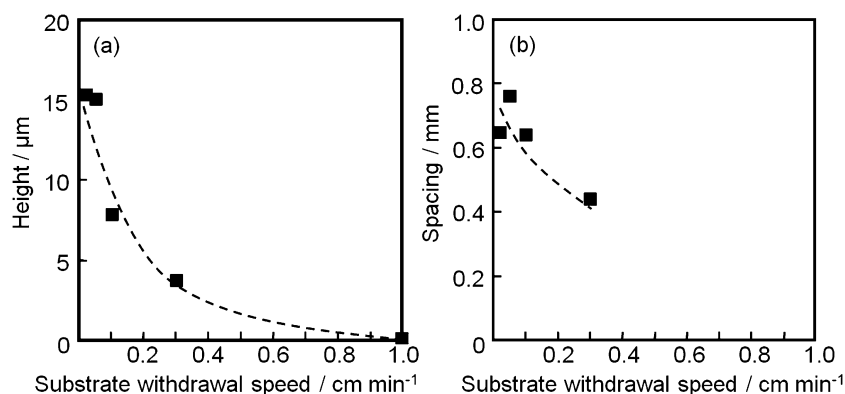


Fig. 10. Dependence of the (a) height and (b) spacing on the substrate withdrawal speed for the silica–PVP hybrid films prepared at varying substrate withdrawal speeds of 0.020–1.0  $\text{cm min}^{-1}$ . Reproduced from Ref. 39 with permission from The Royal Society of Chemistry.

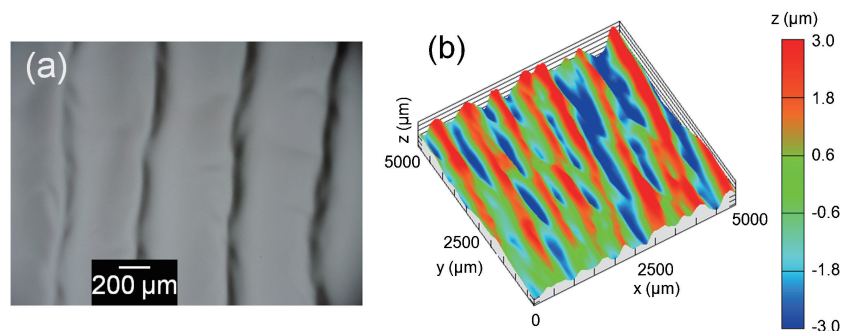


Fig. 12. (a) Optical image and (b) three-dimensional surface profile of the silica-PVP hybrid film prepared at a substrate withdrawal speed of  $0.05 \text{ cm min}^{-1}$  in a thermostatic oven at  $60^\circ\text{C}$ . Reproduced from Ref. 41 with permission from The Royal Society of Chemistry.

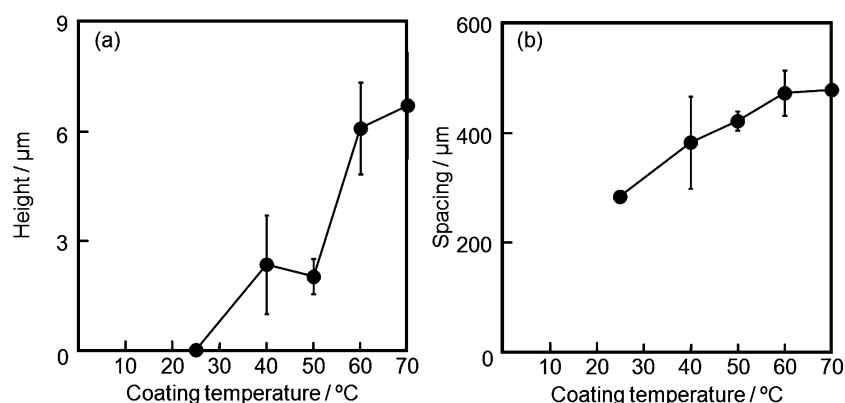


Fig. 13. Dependence of the (a) height and (b) spacing on the coating temperature for the silica-PVP hybrid films prepared at a substrate withdrawal speed of  $0.05 \text{ cm min}^{-1}$  in a thermostatic oven at varying temperatures of  $25\text{--}70^\circ\text{C}$ . Reproduced from Ref. 41 with permission from The Royal Society of Chemistry.

drawal speed of  $0.05 \text{ cm min}^{-1}$  using a dip-coater (PORTABLE DIP COATER DT-0001, SDI, Kyoto, Japan) in a thermostatic oven at varying temperatures of  $25\text{--}70^\circ\text{C}$ . The solutions and substrates were heated at the prescribed temperature for 30 min before the dip-coating process. After deposition, the thin films were kept at room temperature for 24 h in ambient atmosphere.

Transparent, crack-free silica-PVP hybrid films were obtained irrespective of the coating temperature. Increases in the coating temperatures resulted in increases in the film thickness from ca.  $0.36$  to ca.  $11 \mu\text{m}$ . The films prepared at  $25^\circ\text{C}$  featured a smooth surface with inhomogeneities, as inferred from the interference color pattern. In contrast, stripe patterns of  $300\text{--}500 \mu\text{m}$  in spacing, arranged perpendicular to the substrate withdrawal direction, formed at temperatures above  $40^\circ\text{C}$  (Fig. 12). The patterns became more distinct with increasing coating temperatures. Increase in the coating temperature led to increases in the height and spacing of the stripe patterns (Fig. 13).

As described in section 4.2., the spontaneous pattern formation during low-speed dip-coating is attributed to the evaporation-induced capillary flow at the edge of the meniscus. Thus, the rapid solvent evaporation at higher coating temperatures is thought to activate the capillary flow of the coating solution toward the edge of the meniscus, resulting in increases in the height and width of the patterns.

## 5. Concluding remarks

In this review, evaporation-driven self-organization of sol-gel dip-coating films is demonstrated. Convective flows of the coat-

ing layer are triggered by solvent evaporation, resulting in the formation of periodic patterns on the surface of the final gel films. Spontaneous pattern formation induced by Bénard-Marangoni convection occurred upon increase in the substrate withdrawal speeds and coating temperatures. Linear striations and cell-like patterns formed along the flow direction of the coating solution during dip-coating. In contrast, evaporation-driven capillary flow of the coating solution occurred at the meniscus during low-speed dip-coating, generating periodic stripe patterns arranged perpendicular to the substrate withdrawal direction. Such evaporation-driven self-organization process would be useful for the fabrication of highly ordered patterns in inorganic and organic-inorganic thin films.

**Acknowledgements** The author thanks all co-workers for their contributions. This work was financially supported in part by JSPS KAKENHI Grant-in-Aid for Young Scientists (B) (No. 24760554), Izumi Science and Technology Foundation Grant-in-Aid, Iketani Science and Technology Foundation Grant-in-Aid, and The Sumitomo Foundation Grant-in-Aid for Basic Science Research.

## References

- 1) M. H. Stenzel-Rosenbaum, T. P. Davis, A. G. Fane and V. Chen, *Angew. Chem., Int. Ed.*, **40**, 3428–3432 (2001).
- 2) H. Yabu, R. Jia, Y. Matsuo, K. Ijio, S. Yamamoto, F. Nishino, T. Takaki, M. Kuwahara and M. Shimomura, *Adv. Mater.*, **20**, 4200–4204 (2008).
- 3) H. Yabu and M. Shimomura, *Adv. Funct. Mater.*, **15**, 575–581 (2005).

- 4) H. Yabu and M. Shimomura, *Langmuir*, **21**, 1709–1711 (2005).
- 5) T. Ohzono and M. Shimomura, *Langmuir*, **21**, 7230–7237 (2005).
- 6) T. Ohzono and M. Shimomura, *Phys. Rev. E*, **73**, 066140 (2006).
- 7) E. P. Chan and A. J. Crosby, *Adv. Mater.*, **18**, 3238–3242 (2006).
- 8) J. Y. Chung, A. J. Nolte and C. M. Stafford, *Adv. Mater.*, **21**, 1358–1362 (2009).
- 9) M. Takahashi, K. Suzuki, Y. Tokuda, L. Malfatti and P. Innocenzi, *J. Sol-Gel Sci. Technol.*, **70**, 272–277 (2014).
- 10) M. Takahashi, T. Maeda, K. Uemura, J. X. Yao, Y. M. Tokuda, T. Yoko, H. Kaji, A. Marcelli and P. Innocenzi, *Adv. Mater.*, **19**, 4343–4346 (2007).
- 11) S. W. Hong, J. Wang and Z. Q. Lin, *Angew. Chem., Int. Ed.*, **48**, 8356–8360 (2009).
- 12) E. Ishow, R. Camacho-Aguilera, J. Guerin, A. Brosseau and K. Nakatani, *Adv. Funct. Mater.*, **19**, 796–804 (2009).
- 13) O. Karthaus, N. Maruyama, H. Yabu, T. Koito, K. Akagi and M. Shimomura, *Macromol. Symp.*, **160**, 137–142 (2000).
- 14) J. Xu, J. F. Xia and Z. Q. Lin, *Angew. Chem., Int. Ed.*, **46**, 1860–1863 (2007).
- 15) H. Dislich, *Angew. Chem., Int. Ed. Engl.*, **10**, 363–370 (1971).
- 16) I. Strawbridge and P. F. James, *J. Non-Cryst. Solids*, **86**, 381–393 (1986).
- 17) D. P. Birnie, *J. Mater. Res.*, **16**, 1145–1154 (2001).
- 18) D. P. Birnie, III, *Langmuir*, **29**, 9072–9078 (2013).
- 19) D. P. Birnie, D. M. Kaz and D. J. Taylor, *J. Sol-Gel Sci. Technol.*, **49**, 233–237 (2009).
- 20) D. E. Haas and D. P. Birnie, *J. Mater. Sci.*, **37**, 2109–2116 (2002).
- 21) M. Faustini, B. Louis, P. A. Albouy, M. Kuemmel and D. Grosso, *J. Phys. Chem. C*, **114**, 7637–7645 (2010).
- 22) D. Grosso, *J. Mater. Chem.*, **21**, 17033–17038 (2011).
- 23) N. L. Zhang and D. F. Chao, *Int. Commun. Heat Mass Transf.*, **26**, 1069–1080 (1999).
- 24) H. Benard, *Annales De Chimie Et De Physique*, **23**, 62–101 (1901).
- 25) M. J. Block, *Nature*, **178**, 650–651 (1956).
- 26) H. Jeffreys, *Philos. Mag.*, **2**, 833–844 (1926).
- 27) E. L. Koschmieder and M. I. Biggerstaff, *J. Fluid Mech.*, **167**, 49–64 (1986).
- 28) L. Rayleigh, *Philos. Mag.*, **32**, 529–546 (1916).
- 29) J. R. A. Pearson, *J. Fluid Mech.*, **4**, 489–500 (1958).
- 30) H. Kozuka, *J. Ceram. Soc. Japan*, **111**, 624–632 (2003).
- 31) H. Kozuka and M. Hirano, *J. Sol-Gel Sci. Technol.*, **19**, 501–504 (2000).
- 32) H. Kozuka, Y. Ishikawa and N. Ashibe, *J. Sol-Gel Sci. Technol.*, **31**, 245–248 (2004).
- 33) B. K. Daniels, C. R. Szmada, M. K. Templeton and P. Trefonas III, *Proc. SPIE; Int. Soc. Opt. Eng.*, **631**, 192–201 (1986).
- 34) H. Uchiyama, W. Namba and H. Kozuka, *Langmuir*, **26**, 11479–11484 (2010).
- 35) H. Uchiyama, Y. Mantani and H. Kozuka, *Langmuir*, **28**, 10177–10182 (2012).
- 36) L. Landau and B. Levich, *Acta Physicochimica Urss*, **17**, 42–54 (1942).
- 37) R. D. Deegan, O. Bakajin, T. F. Dupont, G. Huber, S. R. Nagel and T. A. Witten, *Nature*, **389**, 827–829 (1997).
- 38) R. D. Deegan, O. Bakajin, T. F. Dupont, G. Huber, S. R. Nagel and T. A. Witten, *Phys. Rev. E*, **62**, 756–765 (2000).
- 39) H. Uchiyama, M. Hayashi and H. Kozuka, *Rsc Adv.*, **2**, 467–473 (2012).
- 40) H. Uchiyama, R. Sasaki and H. Kozuka, *Colloids Surf., A*, **453**, 1–6 (2014).
- 41) H. Uchiyama, D. Shimaoka and H. Kozuka, *Soft Matter*, **8**, 11318–11322 (2012).
- 42) W. Han, M. Byun, B. Li, X. Pang and Z. Lin, *Angew. Chem., Int. Ed.*, **51**, 12588–12592 (2012).
- 43) J. X. Huang, R. Fan, S. Connor and P. D. Yang, *Angew. Chem., Int. Ed.*, **46**, 2414–2417 (2007).
- 44) P. Innocenzi, L. Malfatti, M. Piccinini, D. Grosso and A. Marcelli, *Anal. Chem.*, **81**, 551–556 (2009).
- 45) D. Kim, S. Jeong, B. K. Park and J. Moon, *Appl. Phys. Lett.*, **89**, 264101 (2006).
- 46) N. L. Liu, Y. Zhou, L. Wang, J. B. Peng, J. A. Wang, J. A. Pei and Y. Cao, *Langmuir*, **25**, 665–671 (2009).
- 47) U. Olgun and V. Sevinc, *Powder Technol.*, **183**, 207–212 (2008).
- 48) G. Pu and S. J. Severtson, *Langmuir*, **24**, 4685–4692 (2008).
- 49) S. Watanabe, K. Inukai, S. Mizuta and M. T. Miyahara, *Langmuir*, **25**, 7287–7295 (2009).
- 50) S. Watanabe, Y. Mino, Y. Ichikawa and M. T. Miyahara, *Langmuir*, **28**, 12982–12988 (2012).
- 51) C. Y. Zhang, X. J. Zhang, X. H. Zhang, X. Fan, J. S. Jie, J. C. Chang, C. S. Lee, W. J. Zhang and S. T. Lee, *Adv. Mater.*, **20**, 1716–1720 (2008).



Hiroaki Uchiyama received his Ph.D. in Engineering at Keio University in 2008. He moved to Kansai University, and became an assistant professor in 2009. He has been working in Kansai University as an associate professor since 2014. His research interest includes crystal growth of inorganic materials, and self-organization of inorganic and organic-inorganic hybrid materials.